Optical Materials: X 16 (2022) 100200

Contents lists available at ScienceDirect

Optical Materials: X

journal homepage: www.journals.elsevier.com/optical-materials-x

Pair vacancy defects in β-Ga_2O_3 crystal: Ab initio study

Abay Usseinov [a], Alexander Platonenko [a,b], Zhanymgul Koishybayeva [a], Abdirash Akilbekov [a], Maxim Zdorovets [a], Anatoli I. Popov [a,b,*]

[a] Faculty of Physics and Technical Sciences, L.N. Gumilyov Eurasian National University, 010008, Nur-Sultan, Kazakhstan
[b] Institute of Solid State Physics, University of Latvia, 8 Kengaraga Str, LV-1063, Riga, Latvia

ARTICLE INFO

Keywords:
Ab initio
β-Ga_2O_3
Pair vacancies
Transition levels
Point defects
Electron-hole recombination

ABSTRACT

Despit many studies dedicated to the defects in β-Ga_2O_3, information about formation processes of complex "donor-acceptor" defects in β-Ga_2O_3 and their energetic characteristics is still very scarce. Meanwhile, complex defects, such as pair vacancies, are often indicated as electrically active centers that can play the role of acceptor defects. We have carried out comparative *ab initio* study of formation energies, as well as optical and thermodynamic transition levels of single and pair vacancies in β-Ga_2O. It was confirmed that single gallium and oxygen vacancies are deep acceptors and deep donors, respectively. In this case, the optical transition levels of single gallium and oxygen vacancies are located in such a way that electrons can easily pass from donors to acceptors. Unlike single vacancies, a pair vacancy has a neutral state due to the location of the acceptor levels above the donor ones. However, if pair vacancies were thermally excited, the transition levels are shifted to ~2.0 eV above the top of the valence band, at which the recombination of electrons and holes become possible, as is observed in the case of single vacancies.

1. Introduction

Despite the long history of research (more than 50 years), the β-Ga_2O_3 crystal remains a highly investigated material due its wide range of potential applications [1,2]. In many respects, scientific interest is supported by a suitable electronic structure of β-Ga_2O_3 and its wide band gap of 4.9 eV [3]. The latter makes the crystal transparent in the visible and near ultraviolet spectrum. Due to this, β-Ga_2O_3 can be used in light-emitting devices [4] and scintillation technology [5–8]. The UV absorption with high photoresponse on GaN/Sn:Ga_2O_3 p-n junction makes it possible to create effective solar blind UV photo detectors [9–12], while high breakdown field of β-Ga_2O_3 crystal (>8 MV/cm) allows use it in power rectifies and power metal-oxide-semiconductor field effect transistors (MOSFETs) [13–15]. Finally, a recent study of Cr^{3+}-doped α- and β-phases of Ga_2O_3 showed good electronic flexibility toward non-contractive measurements of the temperature with suitable sensitivity and resolution [16]. All of these and further technological development as well as tailoring of obtained knowledge to specifications needed for application depends on a deep understanding of the evolution of electronic processes during the dopants introduction and intrinsic defects into a crystal via growth processes or irradiation [17,18].

A wide bandgap makes β-Ga_2O_3 an intrinsic insulator, although it displays a semiconducting behavior when synthesized in reducing conditions. The DC and AC conductivity measurements in single crystals of β-Ga_2O_3 show that the dominant mechanism for migration below 900 K is ionic due to diffusion of oxygens in the lattice [19]. Above 900 K, the conductivity is predominantly electronic [19]. It is shown experimentally that β-Ga_2O_3 belong to non-direct-band-gap crystals with gap ~4.83 eV with valence band maximum at the M-point (1/2,1/2,1/2) [20–22]. A direct Γ-Γ band gap has a slightly higher value of 4.87 eV. The small energy difference between gaps and low probability of indirect transition makes β-Ga_2O_3 an effective direct-band-gap crystal.

Despite many studies dedicated to the defects in β-Ga_2O_3, information about formation processes of complex "donor-acceptor" defects in β-Ga_2O_3 and their energetic characteristics is still very scarce, even on a theoretical level. Poor theoretical data can be associated, obviously, with the difficulties of modeling complex defects in low-symmetry systems, which requires the use of large crystal cells and, consequently, makes the *ab initio* calculations expensive in terms of computer resources [23]. Meanwhile, these quantities play a crucial role in explanation of many defect properties. The inability of direct correlation the defects energy characteristics with experimental data brings to the forefront a question about how each point defect and their complexes interplay in the luminescence mechanism.

* Corresponding author. Institute of Solid State Physics, University of Latvia, 8 Kengaraga Str, LV-1063, Riga, Latvia.
E-mail address: popov@latnet.lv (A.I. Popov).

https://doi.org/10.1016/j.omx.2022.100200
Received 29 August 2022; Received in revised form 1 October 2022; Accepted 3 October 2022
Available online 13 October 2022

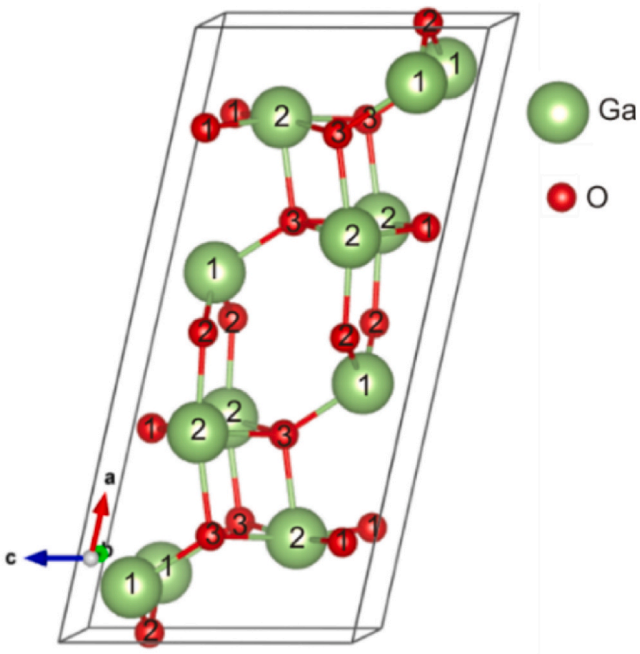

Fig. 1. Atomic model of unit cell of β-Ga_2O_3 (unique positions of Ga and O atoms are denoted).

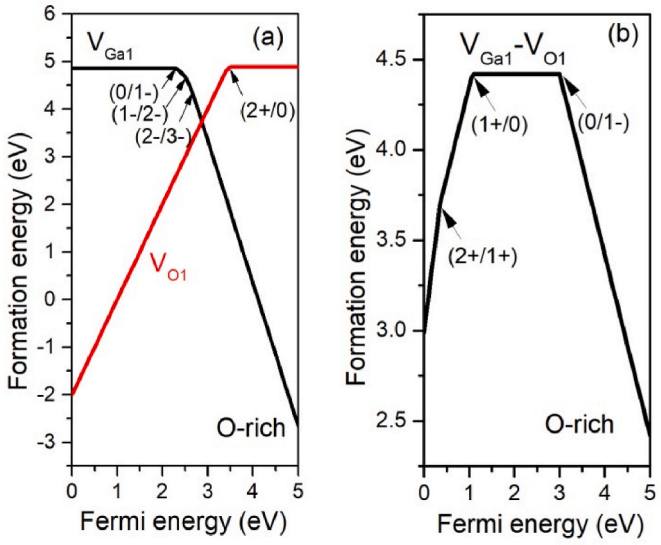

Fig. 2. Formation energy of single V_{Ga1},V_{O1} vacancies (a) and V_{Ga1}-V_{O1} pair vacancy (b) plotted against the Fermi energy at oxygen-rich conditions.

In this work, we focused our efforts on study of the energetic characteristics and electronic structure of single and pair vacancy defects (divacancies) in a β-Ga_2O_3 crystal via calculation the formation energies of considered defects at different charge states and determination of their optical/thermodynamic transition levels. As known, pair vacancy defects are consisting of one gallium and one oxygen vacancies. We considered all possible combinations of V_{Ga}-V_O pair defects in terms of unique site occupation by gallium/oxygen atoms in the monoclinic lattice of β-Ga_2O_3 crystal.

2. Computational details

We calculated formation energy and charge transition levels (optical/thermodynamic) of considered defects employing CRYSTAL17 code [24] using DFT-LCAO approach. Details of the calculation of the defect formation energy and optical transition levels as a function of the Fermi energy and the charge state can be found in our previous work [25]. Additionally, we have calculated the thermodynamic transition levels which are determined from the optical transition levels, taking into account the complete relaxation of the charged defective crystal structure [26]:

$$\varepsilon_{therm} = \varepsilon_{opt} \pm E_{rel} \quad (1)$$

where ε_{opt} is the optical transition level and E_{rel} is the relaxation energy calculated as the difference between the total energies of the charged defect system in the relaxed state and the same charged defect system corresponding to the atomic configuration of the relaxed neutral defect system. At this, in the case of the (1+/0) transition, the relaxation energy has a positive value, and in the case of (0/1–) a negative value (see Fig. 1 and Fig. 2 in Ref. [26] and explanatory text for details).

The basis sets of local functions (BS) for Ga and O atoms were taken from Refs. [27,28], respectively. All calculations have been performed using non-local hybrid B3PW functional [29,30]. For SCF procedure, the cut-off limits in evaluation of Coulomb and exchange series have been chosen to 10^{-7}, 10^{-7}, 10^{-7}, 10^{-7} and 10^{-14} for calculations of the Coulomb overlap, Coulomb penetration, exchange overlap, first exchange pseudo-overlap and second exchange pseudo-overlap integrals, respectively. Total energy difference between two SCF steps (10^{-7} a.u.) also has a high tolerance of accuracy. The effective atomic charges were calculated using the Mulliken population analysis [31]. The integration of the reciprocal space of defect system was performed with a Pack-Monkhorst 2 × 2 × 2 grid [32] resulting in 8 k-points.

To simulate formation of defects in β-Ga_2O_3 crystal, the periodic model of extended unit cell (supercell) were used, all calculations have been performed within 160 atoms supercell with 1 × 4 × 2 expansion matrix. To create vacancies, we removed corresponding oxygen and gallium atoms from their regular positions. We considered the pair defects in which gallium and oxygen vacancies are the nearest neighbor.

Table 1
Calculated and experimental lattice parameters (*a*,*b*,*c*), band gap (E_g), and average high frequency (ε^{∞}) and static (ε^0) dielectric constants.

Property	B3PW	GGA [33]	HSE06 [33]	HSE06 [20]	Exp
a, Å	12.28	12.44	12.25	12.25	12.12 ÷ 12.34 [34]
b, Å	3.05	3.083	3.03	3.05	3.03 ÷ 3.04 [34]
c, Å	5.82	5.876	5.78	5.84	5.80 ÷ 5.87 [34]
E_g, eV	4.89	2.0	4.7	4.87	4.9 [3]
ε^{∞}(average)	3.4	–	–	–	3.57; 3.38; 3.53 [21]
ε^0(average)	9.73	–	–	–	10.2 [35]

3. Results and discussion

3.1. Pure β-Ga2O3

β-Ga_2O_3 crystal has a monoclinic phase with c2/m symmetry. Due to the low symmetry of the crystal, there are two unique positions of Ga atoms (tetrahedral and octahedral) and three positions of O atoms (three- and fourfold coordinated) as denoted in Fig. 1. Tetrahedral and octahedral gallium atoms signed as Ga1 and Ga2, respectively, while two three-coordinated and one four-coordinated oxygen atoms denoted as O1, O2 and O3, respectively. The Ga–O bond lengths range from 1.8 to 2.1 Å.

We have calculated the some basic physical properties of ideal bulk β-Ga_2O_3 that summarized in Table 1 with other theoretical data and experiment. On the whole all properties in good convergence with observed one. It is important to note, that a correct description of the electronic structure, in particular band gap value, play crucial role to

Table 2
Calculated incorporation, relaxation and formation energies (in eV) of vacancy defects in β-Ga_2O_3. Oxygen-rich conditions are used.

Defect	E_{lat}	E_{rel}	E_f	Defect	E_{lat}	E_{rel}	E_f
V_{Ga1}	5.6	−0.8	4.8	V_{O1}	5.5	−0.6	4.9
V_{Ga2}	7	−1.1	5.9	V_{O2}	4.3	−0.1	4.2
				V_{O3}	5.2	−0.1	5.1

Table 3
Calculated formation energy of V_{Ga}-V_O complexes (in eV). Oxygen-rich conditions are used.

Defect	E_{lat}	E_{rel}	E_f	Defect	E_{lat}	E_{rel}	E_f
V_{Ga1}-V_{O1}	6.9	−2.5	4.4	V_{Ga2}-V_{O1}	8.4	−3.0	5.4
V_{Ga1}-V_{O2}	7.4	−2.4	5.0	V_{Ga2}-V_{O2}	9.4	−2.6	6.8
V_{Ga1}-V_{O3}	7.3	−2.4	4.9	V_{Ga2}-V_{O3}	9.0	−3.1	5.9

obtain proper charged defect formation energy. Our computed band gap is in reasonable agreement with the experimentally observed value about 4.9 eV and other hybrid calculated values (Table 1).

3.2. Single and pair vacancy defects in β-Ga2O3

We calculated the formation energy of single V_{Ga} and V_O vacancies under oxygen-rich conditions (Table 2). As is known, the appearance of a defect in a lattice leads to the rising of stresses and, consequently, forces that try to return the system to an equilibrium state. As a result, the atomic structure is rearranged. Therefore, an important indicator of the process of formation of a particular defect is the relaxation energy. It is clear that when the relaxation energy is lower, the atomic structure with a defect is less distorted, and then its formation seems to be more probable. The relaxation energy can be found by dividing the formation energy into two parts: a) the energy of defect incorporation into the unrelaxed crystal lattice (E_{lat}) and the relaxation energy (E_{rel}) due to the relaxation of the crystal structure in the process of complete optimization of the atomic structure (see Table 2) [33].

In general, as follows from Table 2, the formation of all V_O vacancies is an energetically more favorable than the formation of V_{Ga} vacancies under equilibrium conditions. At the same time, the formation energies of V_O vacancies are close to each other, while the formation energies for V_{Ga} vacancies differ significantly (Table 2). Obviously, the strong difference in the formation energies of V_{Ga} vacancies is due to the different coordination of Ga atoms in unique positions (see Fig. 1) and, consequently, the asymmetry of the electronic structure. The same is observed for lattice relaxation: the relaxation near V_O vacancies is smaller than near V_{Ga} vacancies. The low lattice relaxation near V_O vacancies indicates better stability of the system after the formation of a defect. The results obtained well explain the n-type conductivity observed in practice in pure β-Ga_2O_3 crystals, which is possible due to the formation of a sufficient number of V_O vacancies as an electron source. The calculation results are in good agreement with other known theoretical calculations [20,33,36] and agree with experimental observations [19,37].

As the next step, we are considered pair V_{Ga}-V_O defects. Since the odd number of electrons remains after removing of the Ga and O atoms from lattice, a two cases of spin state can be occur: low spin state with s = 1/2 and high spin state with s = 3/2. Thus, we have done a test calculations in order to determine the prefer spin state of neutral V_{Ga}-V_O complexes in β-Ga_2O_3. We have obtain that the low spin state with s = 1/2 for all V_{Ga}-V_O vacancies is energetically more preferable than high spin state with s = 3/2 by considerable value of ~2.8 eV. We suggested that low spin state are cause well-known nature of V_{Ga}, which act as compensating center for donors, thus preventing electronic conductivity. Recently, we have shown that V_{Ga} is a deep acceptor in β-Ga_2O_3 which can compensate donors-like defects [25]. This was in good agreement with many previous theoretical investigations devoted to study of the

Table 4
Optical and thermodynamic transition levels (in eV).

Defect	Transition	ε_{opt}	ε_{therm}	E_{rel}
V_{Ga1}	(0/1-)	2.4	1.86	0.54
	(1-/2-)	2.6	1.97	0.63
	(2-/3-)	2.7	1.7	1.0
V_{O1}	(2+/0)	3.5	4.9	1.4
V_{Ga1}-V_{O1}	(2+/1+)	0.4	1.32	0.92
	(1+/0)	1.1	1.99	0.89
	(0/1-)	3.0	1.89	1.11

vacancy defects in β-Ga_2O_3. Indeed, the electrons, which passed from V_O to V_{Ga}, can "heal" dangling bonds of V_{Ga} with neighbor oxygens, thus lowering the spin state from 3/2 to 1/2 as well as system total energy.

For pair V_{Ga}-V_O vacancies, we calculated the same parameters shown in Table 2. The results are shown in Table 3. As already mentioned, V_{Ga}-V_O complexes are composed of a combination of vacancies in terms of unique atomic positions in a monoclinic lattice. Thus, we have modeled 6 configurations of pair vacancies. It can be seen from the data that the formation of V_{Ga1}-$V_{O(1,2,3)}$ complexes is energetically more preferable than analogous V_{Ga2}-$V_{O(1,2,3)}$ complexes, which, as noted earlier for single defects, is associated with higher coordination of the Ga2 atom and, correspondingly, a higher binding energy in the lattice.

Meanwhile, it should be noted that the formation energies of V_{Ga}-V_O pair vacancies are comparable with the formation energies of single vacancies (Table 2) and may well be formed along with single vacancies. According to Vasil'tsiv et al. [38], the pair V_{Ga}-V_O vacancies are charge-active centers that can play the role of acceptors together with single Ga vacancies. Binet et al. [39] also agrees with the suggestion of Vasil'tsiv et al., and believe that instead of the formation of a high charge state of the V_{Ga}, the formation of a pair V_{Ga}-V_O vacancies is more likely.

Fig. 2 shows the calculated charge transition levels for single V_{Ga1} and V_{O1} vacancies, as well as for the V_{Ga1}-V_{O1} pair vacancy. Given a large number of possible types of pair vacancies and associated with its cumbersomeness of calculations, we limited ourselves to calculating only one lowest-energy configuration of the V_{Ga1}-V_{O1} pair vacancy (see Table 3), and the corresponding single vacancies. The obtained optical transition levels of single vacancies V_{Ga1} and V_{O1} are in good agreement with our recent results on calculations of single defects in β-Ga_2O_3 [25,36], as well as with the results of many similar works [20,34,37,40]. The V_{Ga1} vacancy is a deep acceptor with $\varepsilon(0/1–) = 2.4$ eV, $\varepsilon(1–/2–) = 2.6$, $\varepsilon(2–/3– = 2.7$ eV, while V_{O1} vacancy is a deep donor with $\varepsilon(2+/0) = 3.5$ eV. The V_{O1} acts as a *negative-U* defect, in which the 1+ charge state is energetically unstable [41]. Despite the large depth of single vacancy levels, V_O donor levels can compensate for V_{Ga} acceptor levels, so the energetically stable states for V_O and V_{Ga} in β-Ga_2O_3 are 2+ and 3– states, respectively.

In addition to the neutral state, V_{Ga1}-V_{O1} pair vacancies can have five charge states 1–, 2–, 3–, 1+, 2+. However, not all of these states can arise as a result of a change in the Fermi energy in the band gap. Calculations showed that the V_{Ga1}-V_{O1} pair vacancy is charged as 2+, 1+ and 1– while the remaining 2– and 3– states are unstable. Calculated optical transition levels of the V_{Ga1}-V_{O1} pair vacancy are $\varepsilon(2+/1+) = 0.4$ eV, $\varepsilon(1+/0) = 1.1$ eV and $\varepsilon(0/1–) = 3$ eV. Thus, the V_{Ga1}-V_{O1} pair vacancy is both a deep donor and a deep acceptor. However, unlike single V_{Ga1} and V_{O1} vacancies, the optical transition levels of the V_{Ga1}-V_{O1} pair vacancy lie closer to the edges of the conduction and valence bands. As a result, the probability of spontaneous recombination of a hole at the acceptor level with an electron at the donor level is very low. The proximity of the levels positions to the edges of fundamental bands, as well as the low formation energy of V_{Ga}-V_O pair vacancies, confirm the hypothesis of Vasil'tsiv et al. [38] that V_{Ga}-V_O pair vacancies can play the role of deep acceptors at high Fermi levels. At the same time, the presence of deep donor levels near the top of the valence band (at a depth of >4 eV from the bottom of the conduction band) indicates that

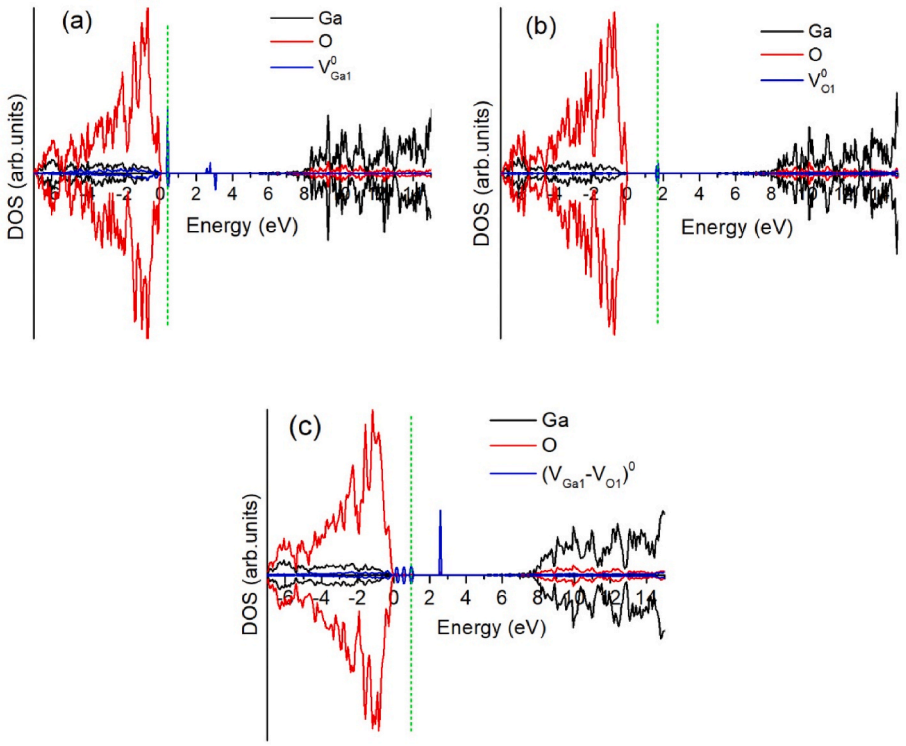

Fig. 3. Total density of states for (a) V^0_{Ga1}, (b) V^0_{O1} and (c) $(V_{Ga1}\text{-}V_{O1})^0$ (see Fig. 1). All defects states in band gap region have been magnified by a factor 5. Green-dashed-vertical lines represent the Fermi level. (For interpretation of the references to colour in this figure legend, the reader is referred to the Web version of this article.)

V_{Ga}-V_O pair vacancies can act as hole sources upon excitation both at the fundamental absorption edge of 4.9–5.0 eV and upon intraband excitations with an energy of ~4.7 eV [39].

In addition to optical transition levels, we have calculated thermodynamic transition levels (Table 4). The thermodynamic levels correspond to the thermal ionization energy of the defect center. In contrast to optical levels, the thermodynamic levels of single V_{Ga1} and V_{O1} vacancies are shifted closer to the edges of valence and conduction bands, respectively. At same time, for the V_{Ga1}-V_{O1} pair vacancy the opposite picture is observed - the thermodynamic levels are located closer to the center of the band gap, around 2 eV above the top of the valence band. The shifting of thermodynamic levels for V_{Ga1}-V_{O1} pair vacancy causes that now levels are located in the band gap in such a way that the recombination of electrons from donor levels with holes at acceptor levels is enabled since now the acceptor level lies below the donor level. In other words, at thermal excitation of the V_{Ga1}-V_{O1} pair vacancy, its action is similar to the action of two single gallium and oxygen vacancies, in which the pair vacancy becomes charged as V^{3-}_{Ga1}-V^{2+}_{O1}. However, in the case of optical transitions, the positive and negative charges on the pair vacancy do not spontaneously recombine and the vacancies remain neutral (V^0_{Ga1}-V^0_{O1}).

Fig. 3 shows the density of states of single V_{Ga1}, V_{O1} vacancies, and V_{Ga1}-V_{O1} pair vacancy. The defects in the crystal lattice leads to the following changes: (i) for the β-Ga_2O_3 lattice with one neutral V_{Ga1} vacancy, the defect states are just at the top of the valence band (VBM), and for the V_{O1} vacancy it is 1.6 eV above VBM. (ii) the appearance of a V_{Ga1}-V_{O1} pair vacancy leads to defect levels 1.3 eV above VBM. The empty levels of the V_{Ga1} vacancy are located approximately in the middle of the band gap, while the occupied levels of the V_{O1} vacancy are located deep from the bottom of the conduction band near the top of the valence band (Fig. 3 a,b). The density of states of the V_{Ga1}-V_{O1} pair vacancy showed that the band gap contains both occupied and unoccupied defect states, which are determined by the states of the oxygen and gallium vacancies, respectively. The occupied levels of the V_{Ga1}-V_{O1} pair vacancy lie at a height of ~1 eV from the VBM, while the unoccupied levels are located even higher, at a height of 2.8 eV.

Before proceeding to the conclusion, it should be noted that these calculations are helpful for the analysis and will facilitate understanding of vacancy defects in more complex oxide compounds based on Ga_2O_3, such as $BaGa_2O_4$ [42,43], $ZnGa_2O_4$ [44,45] and $MgGa_2O_4$ [46,47]. It is important to note that in oxides with a wider energy gap Eg, such as MgO, Al_2O_3, $MgAl_2O_4$, etc., another designation of vacancy defects with trapped electrons is widely used. In particular, an oxygen vacancy in such ionic oxides can have three charge states: a bare oxygen vacancy, as well as vacancies with one or two trapped electrons, which are designated as a one-electron F^+ -center and two-electron *F*-center [48–51]. On the other hand, isolated cationic vacancies can capture one or even two holes, and the hole defects formed in this process are denoted as V^- and V^o centers [52–54].

4. Conclusions

In this work, we present the results of the *ab initio* hybrid DFT calculations on the formation energy and transition levels of single and pair vacancies in β-Ga_2O_3 depending on the charge state and Fermi energy in the band gap. To calculate the defects, we used the B3PW hybrid functional together with the all-electron basis set of the linear combinations of atomic orbitals (LCAO). The results of calculations of the some basic properties of bulk β-Ga_2O_3 showed good agreement with the known experimental data and the results of other theoretical and computational works.

It was shown that the formation of oxygen vacancies is energetically more preferable than the formation of gallium vacancies. This well explains the observed n-type conductivity, which arises due to the accumulation of oxygen vacancies as sources of electrons. V_{Ga}-V_O pair vacancies in the neutral state have a low-spin state $s_z = 1/2$ due to the transfer of electrons from V_O to V_{Ga}. It was shown that pair vacancies can be formed along with single vacancies due comparable formation

energies. Among all combinations of paired vacancies, the creation of V_{Ga1}-$V_{O(1,2,3)}$ complexes is energetically more favorable than similar V_{Ga2}-$V_{O(1,2,3)}$ complexes. The calculated optical and thermodynamic transition levels of single V_{Ga} and V_O vacancies showed that, under equilibrium conditions, V_O vacancies are in the 2+ state, while V_{Ga} vacancies are in the 3– state. In the case of V_{Ga}-V_O pair vacancies, the optical and thermodynamic levels differ significantly. When V_{Ga}-V_O pair vacancies are excited optically, they are stable deep donor-acceptor defects without the effect of charge recombination. Thermal excitation of V_{Ga}-V_O pair vacancies shifts the positions of donor and acceptor levels to the center of the band gap in such a way that recombination of electrons and holes becomes enabled, as is observed in the case of single vacancies. The calculated densities of states for all considered vacancy defects confirm our conclusions about their role in the electronic and optical properties.

CRediT authorship contribution statement

Abay Usseinov: Investigation, Validation, Visualization, Data curation, Writing – review & editing, Project administration. **Alexander Platonenko:** Investigation, Validation, Visualization, Data curation, Writing – review & editing. **Zhanymgul Koishybayeva:** Investigation, Validation, Data curation. **Abdirash Akilbekov:** Investigation, Validation. **Maxim Zdorovets:** Conceptualization, Methodology, Investigation. **Anatoli I. Popov:** Conceptualization, Methodology, Writing – review & editing.

Declaration of competing interest

The authors declare that they have no known competing financial interests or personal relationships that could have appeared to influence the work reported in this paper.

Data availability

Data will be made available on request.

Acknowledgments

This research was funded by the Science Committee of the Ministry of Education and Science of the Republic of Kazakhstan (Grant No. AP08856540).

This research was partly performed at the Institute of Solid State Physics, University of Latvia (ISSP UL). ISSP UL as the Centre of Excellence has received funding from the European Union's Horizon 2020 Framework Programme H2020-WIDESPREAD01-2016-2017-Teaming Phase2 under grant agreement No. 739508, project CAMART2.

References

[1] S.J. Pearton, J. Yang, P.H. Cary, F. Ren, J. Kim, M.J. Tadjer, M.A. Mastro, A review of Ga2O3 materials, processing, and devices, Appl. Phys. Rev. 5 (2018), 011301, https://doi.org/10.1063/1.5006941.

[2] M.A. Mastro, A. Kuramata, J. Calkins, J. Kim, F. Ren, S.J. Pearton, Perspective—opportunities and future directions for Ga2O3, ECS J. Solid State Sci. Technol. 6 (2017) 356–359, https://doi.org/10.1149/2.0031707jss.

[3] M. Orita, H. Ohta, M. Hirano, H. Hosono, Deep-ultraviolet transparent conductive β-Ga2O3 thin films, Appl. Phys. Lett. 77 (2000) 4166–4168, https://doi.org/10.1063/1.1330559.

[4] Z. Galazka, β-Ga2O3 for wide-bandgap electronics and optoelectronics, Semicond. Sci. Technol. 33 (2018), 113001, https://doi.org/10.1088/1361-6641/AADF78.

[5] A. Luchechko, V. Vasyltsiv, Y. Zhydachevskyy, M. Kushlyk, S. Ubizskii, A. Suchocki, Luminescence spectroscopy of Cr3+ ions in bulk single crystalline β-Ga2O3, J. Phys. Appl. Phys. 53 (2020), 354001, https://doi.org/10.1088/1361-6463/AB8C7D.

[6] Y. Usui, T. Oya, G. Okada, N. Kawaguchi, T. Yanagida, Ce-doped Ga2O3 single crystalline semiconductor showing scintillation features, Optik 143 (2017) 150–157, https://doi.org/10.1016/j.ijleo.2017.06.061.

[7] W. Drozdowski, M. Makowski, M.E. Witkowski, A.J. Wojtowicz, Z. Galazka, K. Irmscher, R. Schewski, β-Ga2O3:Ce as a fast scintillator: an unclear role of cerium, Radiat. Meas. 121 (2019) 49–53, https://doi.org/10.1016/j.radmeas.2018.12.009.

[8] A. Luchechko, V. Vasyltsiv, L. Kostyk, O. Tsvetkova, A.I. Popov, Shallow and deep trap levels in X-ray irradiated β-Ga2O3: Mg, Nucl. Instrum. Methods Phys. Res. Sect. B Beam Interact. Mater. Atoms 441 (2019) 12–17, https://doi.org/10.1016/j.nimb.2018.12.045.

[9] C. Sun, D. Guo, G. Wang, H. Liu, H. Yan, L. Li, P. Li, W. Tang, X. Guo, Y. An, Z. Wu, Fabrication of β-Ga2O3 thin films and solar-blind photodetectors by laser MBE technology, Opt. Mater. Express 4 (2014) 1067–1076, https://doi.org/10.1364/OME.4.001067.

[10] W. Li, X. Zhao, Y. Zhi, X. Zhang, Z. Chen, X. Chu, H. Yang, Z. Wu, W. Tang, Fabrication of cerium-doped β-Ga2O3 epitaxial thin films and deep ultraviolet photodetectors, Appl. Opt. 57 (2018) 538, https://doi.org/10.1364/ao.57.000538.

[11] D. Guo, Q. Guo, Z. Chen, Z. Wu, P. Li, W. Tang, Review of Ga2O3-based optoelectronic devices, Mater. Today Phys. 11 (2019), 100157, https://doi.org/10.1016/J.MTPHYS.2019.100157.

[12] D. Guo, Y. Su, H. Shi, P. Li, N. Zhao, J. Ye, S. Wang, A. Liu, Z. Chen, C. Li, W. Tang, Self-powered ultraviolet photodetector with superhigh photoresponsivity (3.05 A/W) based on the GaN/Sn:Ga2O3 pn junction, ACS Nano 12 (2018) 12827–12835, https://doi.org/10.1021/acsnano.8b07997.

[13] G. Kresse, J. Furthmüller, Efficient iterative schemes for ab initio total-energy calculations using a plane-wave basis set, Phys. Rev. B 54 (1996), 11169, https://doi.org/10.1103/PhysRevB.54.11169.

[14] J.B. Varley, A. Schleife, Bethe–Salpeter calculation of optical-absorption spectra of In2O3 and Ga2O3, Semicond. Sci. Technol. 30 (2015), 024010, https://doi.org/10.1088/0268-1242/30/2/024010.

[15] M.J. Tadjer, Cheap ultra-wide bandgap power electronics? Gallium oxide may hold the answer, Electrochem. Soc. Interface 27 (2018) 49–52, https://doi.org/10.1149/2.f05184if.

[16] M. Back, J. Ueda, H. Nambu, M. Fujita, A. Yamamoto, H. Yoshida, H. Tanaka, M. G. Brik, S. Tanabe, Boltzmann thermometry in Cr3+-doped Ga2O3 polymorphs: the structure matters, Adv. Opt. Mater. 9 (2021), https://doi.org/10.1002/ADOM.202100033.

[17] W. Ai, L. Xu, S. Nan, P. Zhai, W. Li, Z. Li, P. Hu, J. Zeng, S. Zhang, L. Liu, Y. Sun, J. Liu, Radiation damage in β-Ga2O3 induced by swift heavy ions, Jpn. J. Appl. Phys. 58 (2019), 120914, https://doi.org/10.7567/1347-4065/AB5599.

[18] E. Farzana, M.F. Chaiken, T.E. Blue, A.R. Arehart, S.A. Ringel, Impact of deep level defects induced by high energy neutron radiation in β-Ga2O3, Apl. Mater. 7 (2019), 022502, https://doi.org/10.1063/1.5054606.

[19] T. Harwig, G.J. Wubs, G.J. Dirksen, Electrical properties of β-Ga2O3 single crystals, Solid State Commun. 18 (1976) 1223–1225, https://doi.org/10.1016/0038-1098(76)90944-3.

[20] J.B. Varley, J.R. Weber, A. Janotti, C.G. Van De Walle, Oxygen vacancies and donor impurities in β-Ga2O3, Appl. Phys. Lett. 97 (2010), 142106, https://doi.org/10.1063/1.3499306.

[21] H. He, R. Orlando, M.A. Blanco, R. Pandey, E. Amzallag, I. Baraille, M. Rérat, First-principles study of the structural, electronic, and optical properties of Ga2O3 in its monoclinic and hexagonal phases, Phys. Rev. B Condens. Matter 74 (2006) 1–8, https://doi.org/10.1103/PhysRevB.74.195123.

[22] C. Janowitz, V. Scherer, M. Mohamed, A. Krapf, H. Dwelk, R. Manzke, Z. Galazka, R. Uecker, K. Irmscher, R. Fornari, M. Michling, D. Schmeißer, J.R. Weber, J. B. Varley, C.G. Van de Walle, Experimental electronic structure of In2O3 and Ga2O3, New J. Phys. 13 (2011), 085014, https://doi.org/10.1088/1367-2630/13/8/085014.

[23] M.A. Blanco, M.B. Sahariah, H. Jiang, A. Costales, R. Pandey, Energetics and migration of point defects in Ga2O3, Phys. Rev. B Condens. Matter 72 (2005), 184103, https://doi.org/10.1103/PhysRevB.72.184103.

[24] R. Dovesi, A. Erba, R. Orlando, C.M. Zicovich-Wilson, B. Civalleri, L. Maschio, M. Rérat, S. Casassa, J. Baima, S. Salustro, B. Kirtman, Quantum-mechanical Condensed Matter Simulations with CRYSTAL, vol. 8, Wiley Interdisciplinary Reviews: Computational Molecular Science, 2018, e1360, https://doi.org/10.1002/WCMS.1360.

[25] A. Usseinov, Z. Koishybayeva, A. Platonenko, V. Pankratov, Y. Suchikova, A. Akilbekov, M. Zdorovets, J. Purans, A.I. Popov, Vacancy defects in Ga2O3: first-principles calculations of electronic structure, Materials 14 (2021) 7384, https://doi.org/10.3390/MA14237384.

[26] F. Gallino, G. Pacchioni, C. Di Valentin, Transition levels of defect centers in ZnO by hybrid functionals and localized basis set approach, J. Chem. Phys. 133 (2010), 144512, https://doi.org/10.1063/1.3491271.

[27] R. Pandey, J.E. Jaffe, N.M. Harrison, Ab initio study of high pressure phase transition in GaN, J. Phys. Chem. Solid. 55 (1994) 1357–1361, https://doi.org/10.1016/0022-3697(94)90221-6.

[28] M.D. Towler, N.L. Allan, N.M. Harrison, V.R. Saunders, W.C. MacKrodt, E. Aprà, Ab initio study of MnO and NiO, Phys. Rev. B 50 (1994) 5041–5054, https://doi.org/10.1103/PhysRevB.50.5041.

[29] A.D. Becke, Density-functional thermochemistry. III. The role of exact exchange, J. Chem. Phys. 98 (1993) 5648–5652, https://doi.org/10.1063/1.464913.

[30] J.P. Perdew, W. Yue, Accurate and simple density functional for the electronic exchange energy: generalized gradient approximation, Phys. Rev. B 33 (1986) 8800, https://doi.org/10.1103/PhysRevB.33.8800.

[31] R.S. Mulliken, Electronic population analysis on LCAO-MO molecular wave functions. II. Overlap populations, bond orders, and covalent bond energies, J. Chem. Phys. 23 (1955) 1841–1846, https://doi.org/10.1063/1.1740589.

[32] H.J. Monkhorst, J.D. Pack, Special points for Brillouin-zone integrations, Phys. Rev. B 13 (1976) 5188–5192, https://doi.org/10.1103/PhysRevB.13.5188.

[33] T. Zacherle, P.C. Schmidt, M. Martin, Ab initio calculations on the defect structure of β-Ga2O3, Phys. Rev. B Condens. Matter 87 (2013) 1–10, https://doi.org/10.1103/PhysRevB.87.235206.
[34] J. Ahman, G. Svensson, J. Albertsson, A reinvestigation of β-gallium oxide, Acta Crystallogr. C 52 (1996) 1336–1338, https://doi.org/10.1107/S0108270195016404.
[35] M. Passlack, E.F. Schubert, W.S. Hobson, M. Hong, N. Moriya, S.N.G. Chu, K. Konstadinidis, J.P. Mannaerts, M.L. Schnoes, G.J. Zydzik, Ga2O3 films for electronic and optoelectronic applications, J. Appl. Phys. 77 (1995) 686–693, https://doi.org/10.1063/1.359055.
[36] J.B. Varley, H. Peelaers, A. Janotti, C.G. Van De Walle, Hydrogenated cation vacancies in semiconducting oxides, J. Phys. Condens. Matter 23 (2011), https://doi.org/10.1088/0953-8984/23/33/334212.
[37] K. Bernhardt, M. Fleischer, H. Meixner, Breakthrough in gas sensors: innovative sensor materials open up new markets, Siemens Components 30 (1995) 35–37.
[38] V.I. Vasil'tsiv, Y.M. Zakharko, Y.I. Prim, Nature of the blue and green luminescence bands of β-gallium sesquioxide, Ukr. Fiz. Zh. 33 (1988) 1320.
[39] L. Binet, D. Gourier, Origin of the blue luminescence of β-Ga2O3, J. Phys. Chem. Solid. 59 (1998) 1241–1249, https://doi.org/10.1016/S0022-3697(98)00047-X.
[40] J. Lee, S. Ganguli, A.K. Roy, S.C. Badescu, Density functional tight binding study of β-Ga2O3 : electronic structure, surface energy, and native point defects, J. Chem. Phys. 150 (2019), https://doi.org/10.1063/1.5088941.
[41] M.D. McCluskey, Point defects in Ga2O3, J. Appl. Phys. 127 (2020), 101101, https://doi.org/10.1063/1.5142195.
[42] H. Klym, I. Karbovnyk, A. Luchechko, Y. Kostiv, A.I. Popov, Extended positron trapping defects in the Eu3+-doped BaGa2O4 ceramics studied by PAL method, Phys. Status Solidi 259 (2022), 2100485, https://doi.org/10.1002/pssb.202100485.
[43] H. Klym, I. Karbovnyk, A. Luchechko, Y. Kostiv, V. Pankratova, A.I. Popov, Evolution of free volumes in polycrystalline BaGa2O4 ceramics doped with Eu3+ ions, Crystals 11 (2021) 1515, https://doi.org/10.3390/cryst11121515.
[44] J. Ueda, M. Back, M.G. Brik, Y.X. Zhuang, M. Grinberg, S. Tanabe, Ratiometric optical thermometry using deep red luminescence from 4T2 and 2E states of Cr3+ in ZnGa2O4 host, Opt. Mater. 85 (2018) 510–516.
[45] A. Luchechko, Y. Zhydachevskyy, S. Ubizskii, O. Kravets, A.I. Popov, U. Rogulis, E. Elsts, E. Bulur, A. Suchocki, Afterglow, TL and OSL properties of Mn2+-doped ZnGa2O4 phosphor, Sci. Rep. 9 (2019) 9544, https://doi.org/10.1038/s41598-019-45869-7.
[46] [a] A. Luchechko, Y. Zhydachevskii, D. Sugak, O. Kravets, N. Martynyuk, A. Popov, S. Ubizskii, A. Suchocki, Luminescence properties and decay kinetics of Mn2+ and Eu3+ co-dopant ions in MgGa2O4 ceramics, Latv. J. Phys. Tech. Sci. 55 (2018) 43–51, https://doi.org/10.2478/lpts-2018-0043;
[b] L. Andreici, M.G. Brik, N.M. Avram, Electron-phonon coupling in Ni2+-doped MgGa2O4 spinel, Rom. Rep. Phys. 63 (4) (2011) 1048.
[47] A.I. Popov, E.A. Kotomin, J. Maier, Basic properties of the F-type centers in halides, oxides and perovskites, Nucl. Instrum. Methods Phys. Res. B 268 (2010) 3084–3089.
[48] E.A. Kotomin, A.I. Popov, Radiation-induced point defects in simple oxides, Nucl. Instrum. Methods B 141 (1998) 1–15, https://doi.org/10.1016/S0168-583X(98)00079-2.
[49] A. Popov, M. Monge, R. González, Y. Chen, E. Kotomin, Dynamics of F-center annihilation in thermochemically reduced MgO single crystals, Solid State Commun. 118 (2001) 163–167.
[50] A.I. Popov, E.A. Kotomin, M.M. Kuklja, Quantum chemical calculations of the electron center diffusion in MgO crystals, Phys. Status Solidi 195 (1) (1996) 61–66.
[51] R. González, M.A. Monge, J.E. Muñoz Santiuste, R. Pareja, Y. Chen, E. Kotomin, M. M. Kukla, A.I. Popov, Photoconversion of F-type centers in thermochemically reduced MgO single crystals, Phys. Rev. B 59 (1999) 4786.
[52] S. Dolgov, T. Kärner, A. Lushchik, A. Maaroos, S. Nakonechnyi, E. Shablonin. Trapped- hole centers in MgO single crystals, Phys. Solid State 53 (2011) 1244.
[53] M.A. Monge, R. Gonzalez R, J.E. Munoz Santiuste, R. Pareja, Y. Chen, E. A. Kotomin, A.I. Popov, Photoconversion of F+ centers in neutron-irradiated MgO, Nucl. Instrum. Methods B 166 (2020) 220–224.
[54] Y. Chen, M.M. Abraham, Trapped-hole centers in alkaline-earth oxides, J. Phys. Chem. Solid. 51 (7) (1990) 747–764, https://doi.org/10.1016/0022-3697(90)90147-8.